

Exact and Stable Tip Trajectory Tracking for Multi-Link Flexible Manipulator

Hongchao Zhao Degang Chen
Dept. of Electrical Engineering and Computer Engineering
Iowa State University
Ames, IA 50011

Abstract

In this paper, the recently developed stable inversion theory for nonlinear nonminimum phase systems is applied to output tracking for multi-link flexible robot manipulators. First a mathematical model is developed for a two-link flexible manipulator using assumed mode technique with tip position as output. Then an inverse model is derived and a two-point boundary value problem is set up to guarantee that the inverse obtained is a stable one regardless of the fact that a flexible manipulator is a nonminimum phase system. The eigenvalues of the Jacobian matrix of the inverse system are calculated to verify the hyperbolicity of the fixed point. Following a recent general result, an iterative procedure is presented to numerically construct the stable inverse for a given desired tip trajectory. This inverse is used as a feed forward together with joint angle feedback to control the tip position. Excellent output tracking is achieved with no transient or steady state errors and no internal vibration builds up. This is contrasted with the performance of the well known computed torque method where large tracking errors such as undershoot, overshoot, and oscillation exist.

1 Introduction

Research interest in the control of articulated flexible structures has considerably increased in the past few years, as evidenced by the large number of such papers at recent CDC's and ACC's. This is motivated by the need for space-based manipulators which are necessarily lightweight and therefore flexible, due to the high transportation cost. The expense of large motors and amplifiers required to drive massive earth-bound industrial manipulators is additional motivation for the design and control of lightweight manipulators. Furthermore, even for robot manipulators normally considered to be rigid, link flexibility cannot be neglected during fast speed motion control.

The study of flexible manipulator control was pioneered by Cannon and Schmitz[3] where a linear quadratic optimal control approach was successfully applied to the end-effector tracking control of a one-link flexible robot arm in which the nonminimum phase effect was first demonstrated. After that, many researchers have considered different approaches to the control of one-link flexible arm which is a linear system for small deflections. Among those, Siciliano and Book[9] used a singular perturbation approach to deal with the flexible modes and Bayo[1] applied Fourier transform to obtain stable but noncausal control input.

Nonlinear control of multi-link flexible manipulators is recent and limited. Lucibello Di Benedetto[8] applied the recently developed nonlinear regulation theory to the control of nonlinear flexible arms and the asymptotic tracking of periodic output trajectories was achieved. In a similar approach by De Luca, et al[6], simulation results demonstrated asymptotic tracking of a finite trajectory with transient errors existing at the beginning and at the end of the maneuver. This transient error phenomenon is a fundamental limitation of the regulation approach.

Another approach to output tracking is based on inversion which was first studied by Brockett and Mesarovic[2]. Later on, Silverman[10] developed an easy-to-follow step-by-step procedure for the inversion of multivariable linear systems. The linear inversion results were extended by Hirschorn[7] to real analytic nonlinear systems. Singh[11], for example, had similar results on nonlinear inversion with some modified conditions. All these inversion algorithms produce causal inverses for a given desired output $y_d(t)$ and a fixed initial condition $x(t_0)$, and unbounded $u(t)$ and $x(t)$ were produced for nonminimum phase systems. This fundamental difficulty has been noted for a long time.

Motivated by the success of the noncausal inverse dynamics approach and the difficulties in both classical inversion and recent nonlinear regulation, the notion of stable inversion has recently been developed[5]

and the problem has been solved for a class of nonlinear nonminimum phase systems with well defined relative degree whose zero dynamics has a hyperbolic fixed point. A numerical procedure is also developed[4] for constructing stable inverses based on iterative linearization and decomposition of the stable/unstable subspaces. This approach to output tracking avoids difficulties in both regulation and classical inversion while preserves the advantages of both and is applied to achieve exact tip trajectory tracking for multi-link flexible manipulators in this paper.

2 Solution of Stable Inversion

Consider a nonlinear system of the form

$$\dot{x} = f(x) + g(x)u \quad (1)$$

$$y = h(x), \quad (2)$$

defined on a neighborhood X of the origin of \mathbf{R}^n , with input $u \in \mathbf{R}^m$ and output $y \in \mathbf{R}^m$. $f(x)$ and $g_i(x)$ (the i th column of $g(x)$) for $i = 1, 2, \dots, m$ are smooth vector fields and $h_i(x)$ for $i = 1, 2, \dots, m$ are smooth functions on X with $f(0) = 0$ and $h(0) = 0$. For such a system, the stable inversion problem[4] is stated as follows: Given a smooth reference output trajectory $y_d(t)$ with compact support, find a bounded control input $u_d(t)$ and a bounded state trajectory $x_d(t)$ with $u_d(t) \rightarrow 0$ and $x_d(t) \rightarrow 0$ as $t \rightarrow \pm\infty$ such that $x_d(t)$ and $u_d(t)$ satisfy the system equations (1) and (2).

For systems with well defined relative degree whose zero dynamics has a hyperbolic fixed point, it has been shown[5] that the stable inversion problem has a unique solution and an iterative linearization approach can be followed. Let the system in (1) and (2) has relative degree $r = (r_1, r_2, \dots, r_m)^T \in \mathbf{N}^m$ at the equilibrium point 0. Define $\xi_k^i = y_i^{(k-1)}$ for $i = 1, \dots, m$ and $k = 1, \dots, r_i$, and denote

$$\begin{aligned} \xi &= (\xi_1^1, \xi_2^1, \dots, \xi_{r_1}^1, \xi_1^2, \dots, \xi_{r_m}^m)^T \\ &= (y_1, \dot{y}_1, \dots, y_1^{(r_1-1)}, y_2, \dots, y_m^{(r_m-1)})^T. \end{aligned}$$

Choose η , an $n - \sum_{i=1}^m r_i$ dimensional function on \mathbf{R}^n such that $(\xi^T, \eta^T)^T = \psi(x)$ forms a change of coordinates with $\psi(0) = 0$. In this new coordinate system, the stable inversion problem is shown to be equivalent to the following two point boundary value (TPBV) problem

$$\dot{\eta} = p(y_d^{(r)}, \xi_d, \eta), \quad (3)$$

subject to

$$B^s(\eta(t_0)) = 0, \quad B^u(\eta(t_f)) = 0, \quad (4)$$

where (3) is the so-called reference dynamics, $B^s(\eta) = 0$ characterizes the unstable manifold and $B^u(\eta) = 0$ the stable manifold. Once the TPBV problem is solved, x_d and u_d can be constructed as follows

$$x_d = \psi^{-1}(\xi_d, \eta),$$

$$u_d = (L_g L_f^{r-1} h(\psi^{-1}(\xi_d, \eta)))^{-1} (y_d^{(r)} - L_f^r h(\psi^{-1}(\xi_d, \eta))).$$

The iterative linearization approach to the solution of the TPBV problem is as follows. In each iteration, equations (3) and (4) are linearized along the solution from the previous step to obtain a new linear time varying two point boundary value problem. This linear problem is solved by decoupling the stable and unstable subspaces and integrating the stable part forward in time and the unstable part backward in time. The iteration continues until some convergence criterion is met.

To initialize, we take $\eta_0(t) = 0$ for all t . Let $\eta_k(t)$ be the solution from the previous step. Linearizing the right hand sides of equation (3) and equation (4) along $\eta_k(t)$, we have a linear TPBV problem

$$\dot{\eta} = A(t)\eta + b(t), \quad (5)$$

subject to

$$C_s \eta(t_0) = \alpha, \quad C_u \eta(t_f) = \beta, \quad (6)$$

for some appropriate matrices A , b , C_s , C_u , α and β . To decouple the stable and unstable subspaces, we apply a change of coordinates:

$$z = \begin{bmatrix} z_1 \\ z_2 \end{bmatrix} \stackrel{\text{def}}{=} \begin{bmatrix} C_s \\ C_u \end{bmatrix} \eta,$$

where z_1 is, roughly speaking, the stable part of η , z_2 the unstable part, and they satisfy

$$\dot{z}_1 = A_{11}(t)z_1 + A_{12}(t)z_2 + b_1(t), \quad (7)$$

$$\dot{z}_2 = A_{21}(t)z_1 + A_{22}(t)z_2 + b_2(t), \quad (8)$$

with initial and final conditions specified, respectively, as $z_1(t_0) = \alpha$ and $z_2(t_f) = \beta$. The key to the decoupling is to recognize that the solutions z_1 and z_2 are linearly related as follows

$$z_2(t) = S(t)z_1(t) + g(t), \quad (9)$$

with suitable final value conditions $S(t_f) = 0$ and $g(t_f) = \beta$. It can be further shown that S and g satisfy

$$\dot{S} = A_{21} + A_{22}S - SA_{11} - SA_{12}S, \quad (10)$$

$$\dot{g} = (A_{22} - SA_{12})g + (b_2 - Sb_1). \quad (11)$$

Since equation (10) contains only known functions except S , it can be integrated backward in time to

get $S(t)$. Once this is done, equation (11) can also be integrated backward in time to solve for $g(t)$. With S and g as known functions, equation (7) can be rewritten as

$$\dot{z}_1 = (A_{11}(t) + A_{12}(t)S(t))z_1 + b_1(t) + A_{12}(t)g(t), \quad (12)$$

which can be integrated forward in time to obtain $z_1(t)$. Finally, the algebraic equation (9) is used to obtain $z_2(t)$.

3 Forward Dynamics

A robot can be considered as the assembly of many flexible links. For simplicity, we consider a robot arm with two flexible links. Both joints are revolute and input torques are applied at these points. Each link i has total length l_i , mass per unit length ρ_i , area moment of inertia I_i , Young's modulus E_i . Attached at one end of link i is a tip mass m_{e_i} , and at the other end a hub of inertia I_{h_i} . We assume that the links are maneuvered in the horizontal plane and that the out-of-plane deflections are negligible.

By the assumed modes method we may approximate the continuous deflection of a flexible link by a set of assumed shape functions and their time-dependent generalized coordinates. Let the flexible displacements of link 1 and link 2 be $\delta_1(h_1, t)$ and $\delta_2(h_2, t)$ respectively. Also, let $\phi_{1j}(h_1)$ and $\phi_{2j}(h_2)$ be the j th necessary admissible shape functions of link 1 and link 2 respectively, $q_{1j}(t)$ and $q_{2j}(t)$ be the corresponding generalized coordinates. Then the distributed deflections of the two links are approximated by

$$\delta_i(h_i, t) = \sum_{j=1}^{n_i} \phi_{ij}(h_i) q_{ij}(t) = \phi_i^T q_i, \quad \forall i = 1, 2 \quad (13)$$

In this paper, we take $n_1 = n_2 = 2$.

By using the extended Hamilton's Principle in the form of Lagrange's equations, the equations of motion can be expressed as

$$\frac{d}{dt} \frac{\partial L}{\partial \dot{\psi}} - \frac{\partial L}{\partial \psi} = \tau, \quad (14)$$

where $\psi = (\theta_1, \theta_2, q_{11}, q_{12}, q_{21}, q_{22})^T$ is a set of generalized coordinates for the system; L , the Lagrangian, is the difference between the kinetic energy T and the potential energy P ; and τ is the generalized force acting on the generalized coordinates. In the case of robot arm

$$P = \frac{1}{2} \psi^T K \psi, \quad \text{and} \quad T = \frac{1}{2} \dot{\psi}^T M(\psi) \dot{\psi}, \quad (15)$$

where $M(\psi)$ is a positive definite symmetric inertia matrix and is a nonlinear function of ψ , and K is the

stiffness matrix composed of the stiffness matrices of the flexible links. Substituting (15) into (14) we get

$$M \ddot{\psi} + \dot{M} \dot{\psi} - \frac{1}{2} \frac{\partial(\dot{\psi}^T M \dot{\psi})}{\partial \psi} + K \psi = Bu - d, \quad (16)$$

where $u = (u_1, u_2)^T$ is the input torque vector applied at the joints, $B = [I_{2 \times 2} \quad 0_{2 \times 4}]^T$ determines how joint torques affect the generalized coordinates, and d is the Rayleigh dissipation force due to structural damping of the flexible links which has the form:

$$d = C \dot{\psi}, \quad (17)$$

where C is the damping matrix taken to be a proportion of the stiffness matrix as a common practice. Hence, equation (16) can be written as

$$M \ddot{\psi} + H(\psi, \dot{\psi}) + C \dot{\psi} + K \psi = Bu. \quad (18)$$

There are many ways to choose the system output. Depending on which point along the links the output point is located, the whole system can be either minimum or nonminimum phase. If the output is selected to be the joint angles, i.e. the sensors and actuators are collocated, the system is known to be minimum phase. A more meaningful choice of output, as is our choice, is the tip position. But this choice renders the system nonminimum phase which will be demonstrated later on by the eigenvalues of inverse system. Both the Cartesian coordinates and angular coordinates can be used for tip positions. Here for simplicity, we choose the tip angular positions as the system output, which is given by

$$y = \theta + \left[\arctan\left(\frac{\delta_1(l_1, t)}{l_1}\right), \arctan\left(\frac{\delta_2(l_2, t)}{l_2}\right) \right]^T, \quad (19)$$

where $\theta = (\theta_1, \theta_2)^T$, $y = (y_1, y_2)^T$. For small elastic deformations $\arctan(\cdot)$ can be approximated by (\cdot) and by substituting (13) into equation (19) we obtain

$$y = D \psi, \quad (20)$$

where $D = [D_1 \quad D_2]$, $D_1 = I_{2 \times 2}$, and

$$D_2 = \begin{bmatrix} \frac{\phi_{11}(l_1)}{l_1} & \frac{\phi_{12}(l_1)}{l_1} & 0 & 0 \\ 0 & 0 & \frac{\phi_{21}(l_2)}{l_2} & \frac{\phi_{22}(l_2)}{l_2} \end{bmatrix}.$$

To summarize, we have the forward dynamic equations of the two-link flexible arm described by

$$M(\psi) \ddot{\psi} + H(\psi, \dot{\psi}) + C \dot{\psi} + K \psi = Bu, \quad (21)$$

$$y = D \psi, \quad (22)$$

where all matrices are defined as above.

4 Inverse Dynamics

Based on the above forward dynamic equations, we here derive the linearized inverse dynamic equations. Equation (21) can be written in two parts:

$$M_{11}(\psi)\ddot{\theta} + M_{12}(\psi)\ddot{q} + H_1(\psi, \dot{\psi}) = B_1 u,$$

$$M_{21}(\psi)\ddot{\theta} + M_{22}(\psi)\ddot{q} + H_2(\psi, \dot{\psi}) + M_2\dot{q} + M_3q = 0.$$

Given a reference output trajectory $y_d(t)$, equation (22) can be written as

$$\theta = D_1^{-1}y_d - D_1^{-1}D_2q.$$

Substituting this into the second part of equation (21), we obtain the nonlinear inverse dynamic equation

$$M_1\ddot{q} + M_2\dot{q} + M_3q + H_2(y_d, \dot{y}_d, q, \dot{q}) = M_4\ddot{y}_d, \quad (23)$$

where

$$M_1 = M_{22}(y_d(t), q(t)) - M_{21}(y_d(t), q(t))D_1^{-1}D_2,$$

$$M_4 = -M_{21}(y_d(t), q(t))D_1^{-1}.$$

In order to carry out the iterative algorithm to do the inversion, we need to linearize the inverse dynamic equation (23). Let us do it term by term at point defined as $(q_0^T, \dot{q}_0^T)^T$. For convenience, we write terms only as functions of q 's instead of both q 's and y_d 's.

Let $M(x)$ be a $k \times l$ matrix function of $x \in \mathbf{R}^n$ and $y \in \mathbf{R}^n$ be a column vector. The derivative of M at a point x_0 in the direction of y is defined as

$$D_x^{x_0} M y \stackrel{\text{def}}{=} \sum_{i=1}^n \frac{\partial M}{\partial x_i} \Big|_{x=x_0} y_i.$$

Using this notation and neglecting higher order terms, the first term $M_1(q)\ddot{q}$ in equation (23) can be linearized as

$$\begin{aligned} M_1(q)\ddot{q} &= [M_1^0 + D_q^0 M_1 [q - q_0]] [\ddot{q}_0 + [\ddot{q} - \ddot{q}_0]] \\ &= M_1^0 \ddot{q} + [D_q^0(M_1 q)] \ddot{q}_0 - [D_q^0(M_1 q_0)] \ddot{q}_0, \end{aligned}$$

where the superscript 0 stands for evaluation along q_0 or \dot{q}_0 no matter whichever is applicable. Since it can be easily verified that

$$[D_x(My)]z = [D_x(Mz)]y,$$

where z is an appropriately dimensioned vector or matrix, we obtain

$$M_1(q)\ddot{q} = M_1^0 \ddot{q} + D_q^0(M_1 \ddot{q}_0)q - D_q^0(M_1 \ddot{q}_0)q_0.$$

M_2 and M_3 both are constant matrices. For the term $H_2(q, \dot{q})$, we have

$$\begin{aligned} H_2 &= H_2^0 + D_q^0 H_2 [q - q_0] + D_{\dot{q}}^0 H_2 [\dot{q} - \dot{q}_0] \\ &= H_2^0 - D_q^0 H_2 q_0 - D_{\dot{q}}^0 H_2 \dot{q}_0 + D_q^0 H_2 q + D_{\dot{q}}^0 H_2 \dot{q}. \end{aligned}$$

Similar to the derivation for the first term, we can get the linearized form of $M_4\ddot{y}_d$ as

$$M_4\ddot{y}_d = M_4^0 \ddot{y}_d - D_q^0(M_4 \ddot{y}_d)q + D_q^0(M_4 \ddot{y}_d)q.$$

Thus the linearized inverse dynamics can be expressed as:

$$A_1(q_0)\ddot{q} + A_2(q_0, \dot{q}_0)\dot{q} + A_3(q_0, \dot{q}_0, \ddot{q}_0)q = A_4(q_0, \dot{q}_0, \ddot{q}_0),$$

where

$$\begin{aligned} A_1 &= M_1^0; \\ A_2 &= M_2 + D_q^0 H_2; \\ A_3 &= D_q^0(M_1 \ddot{q}_0) + M_3 + D_q^0 H_2 - D_q^0(M_4 \ddot{y}_d); \\ A_4 &= M_4 \ddot{y}_d - D_q^0(M_4 \ddot{y}_d)q_0 + D_q^0(M_1 \ddot{q}_0)q_0 + \\ &\quad + D_q^0 H_2 q_0 + D_{\dot{q}}^0 H_2 \dot{q}_0 - H_2^0. \end{aligned}$$

The state space form of the inverse dynamics can thus be written as

$$\dot{x}(t) = A(t)x(t) + b(t), \quad (24)$$

where $x = (q^T, \dot{q}^T)^T$, and

$$A(t) = \begin{bmatrix} 0 & I \\ -A_1^{-1}A_3 & -A_1^{-1}A_2 \end{bmatrix} \quad b(t) = \begin{bmatrix} 0 \\ A_1^{-1}A_4 \end{bmatrix}.$$

It is a generally accepted fact that a flexible link manipulator with tip position as output is a nonminimum phase system. Thus its inverse system has eigenvalues in both left and right half planes. In addition, since sustained oscillation without any tip movement is physically impossible, the inverse system has no eigenvalues on the $j\omega$ -axis and thus must have a hyperbolic fixed point. These properties are verified in the next section when the eigenvalues of the inverse system are actually computed.

Let us now form the matrix X_s by taking as columns the eigenvectors and the generalized eigenvectors of $A(t)$ at some fixed time t corresponding to eigenvalues having negative real parts, and X_u , those corresponding to eigenvalues having positive real parts. Then, we have

$$A(t) [X_s \quad X_u] = [X_s \quad X_u] \begin{bmatrix} \Lambda_s & 0 \\ 0 & \Lambda_u \end{bmatrix}, \quad (25)$$

where Λ_s and Λ_u are the corresponding Jordan forms. Denote

$$\begin{bmatrix} Y_s \\ Y_u \end{bmatrix} = [X_s \quad X_u]^{-1}.$$

From (25) we obtain

$$Y_s A(t) X_u = 0, \quad \text{and} \quad Y_u A(t) X_s = 0. \quad (26)$$

Since we know that $x(t)$ belongs to the unstable manifold for all $t \leq t_0$ and $x(t)$ belongs to the stable manifold for all $t \geq t_f$, therefore $x(t_0)$ (resp.

$x(t_f)$) can be written as the linear combination of the columns of X_u (resp. X_s):

$$x(t_0) = X_u Z_u, \quad \text{and} \quad x(t_f) = X_s Z_s. \quad (27)$$

Combining equations (26) and (27), we have

$$Y_s A(t_0) x(t_0) = Y_s A(t_0) X_u Z_u = 0,$$

$$Y_u A(t_f) x(t_f) = Y_u A(t_f) X_s Z_s = 0.$$

Denoting $C_s = Y_s A(t_0)$ and $C_u = Y_u A(t_f)$ we obtain the linear time varying TPBV problem

$$\dot{x}(t) = A(t)x(t) + b(t) \quad (28)$$

subject to

$$C_s x(t_0) = 0, \quad C_u x(t_f) = 0, \quad (29)$$

where all matrices are defined as above.

5 Simulation Analysis

In this section, we present the digital simulation results to illustrate the performance of the inverse dynamics method. The simulation goes through the following iterative procedure:

- Step 1: Set $q_0(t) = 0$ for all t .
- Step 2: Linearize (23) along $q_0(t)$ to get (28) and (7)–(12).
- Step 3: Integrate equation (10) backward in time to get $S(t)$.
- Step 4: Integrate equation (11) backward in time to get $g(t)$.
- Step 5: Integrate equation (12) forward in time to get $z_1(t)$ and get $z_2(t)$ by (9).
- Step 6: Compute $q(t) = \begin{bmatrix} C_s \\ C_u \end{bmatrix}^{-1} \begin{bmatrix} z_1 \\ z_2 \end{bmatrix}$.
- Step 7: If $\|q - q_0\|$ is greater than threshold, then $q_0 = q$ and go to step 2, else continue.
- Step 8: Compute nominal input $u_d(t)$ from the first part of equation (21).

The two-link flexible arm with the properties listed in Table 1 is utilized as the physical model. The eigenvalues of the forward dynamic equations and the inverse dynamic equations are shown in Table 2 from which it can be seen that the system is nonminimum phase and the inverse dynamic system is hyperbolic.

Using the iterative algorithm from step 1 to step 7 we first compute the flexible modes corresponding to the tip trajectories. Then, we compute the required

Parameter	Link One	Link Two
$l(m)$	1.0	1.0
$\rho(kg/m^2)$	0.3	0.1
$EI(Nm^2)$	15.75	1.75
$m_e(kg)$	0.15	0.10
$I_b(kgm^2)$	0.2	0.067

Table 1: Two-Flexible-Link Arm Properties

Forward Dynamics	Inverse Dynamics
0	167.66
0	6.27±10.48i
0	-62.64
0	-6.80±9.19i
-0.62±11.13i	-45.77±84.02i
-1.78±18.77i	
-45.61±83.91i	
-119.49±98.08i	

Table 2: Eigenvalues at $\theta_2 = 90^\circ$

torques by step 8. Fig. 1 shows the joint torques needed to produce the desired tip trajectories. As expected, the torques needs to be applied to preshape the links some time before the tip starts moving.

The calculated torque was applied to the forward dynamic equations. Since we will compare our simulated results with those of computed torque technique, we use the same control structure as that of the computed torque technique. As the results shown in Fig. 2 the tips follow the desired trajectories exactly without any undershoot or overshoot.

Consider a typical method called computed torque technique using only the rigid modes for feedback since flexible modes are assumed not to be measurable. The input torque to the system can be expressed as

$$\tau^* = M(\theta_d)\ddot{\theta}_d + H_1(\theta_d, \dot{\theta}_d) + K_d(\dot{\theta}_d - \dot{\theta}) + K_p(\theta_d - \theta).$$

In requiring the same tip trajectories, as we can expect, the generated output profiles by the computed torque technique exhibit some significant error which includes the obvious undershoot and the overshoot. The simulation results are also shown in Fig. 3.

6 Conclusion

The iterative approach to stable inversion of nonlinear nonminimum phase systems is successfully applied to the tip trajectory tracking for a two-flexible-link robot manipulator. The key assumptions on well defined

relative degree and hyperbolicity of the fixed point of the zero dynamics are satisfied. Simulation results demonstrate that the stable inversion approach is very effective for obtaining exact output tracking for flexible manipulators. This approach is expected to perform equivalently well for other realistic nonminimum phase systems. Future work will be on efficient numerical algorithms for constructing stable inverses and on new applications of stable inversion.

References

[1] Bayo, E., 1987. "A Finite-Element Approach to Control the End-Point Motion of a Single-Link Flexible Robot," *J. Robotic Systems*, vol.4, no.1, pp.63-75.

[2] Brockett, R. W. and Mesarovic, M. D., 1965, "The Reproducibility of Multivariable Systems," *J. Mathematical Analysis and Applications*, vol.11, pp.548-563.

[3] Cannon, R. H., and Schmitz, E., 1984, "Initial Experiments on the End Point Control of a Flexible One-link Robot," *Int. J. Robotics Research*, vol.3, pp.62-75.

[4] Chen, D., 1993, "An Iterative Solution to Stable Inversion of Nonlinear Nonminimum Phase Systems," *Proceedings of American Control Conference*, San Francisco.

[5] Chen, D. and Paden, B., 1992, "Stable Inversion of Nonlinear Nonminimum Phase Systems," *Proceedings of Japan/USA Symposium on Flexible Automation*, pp.791-797.

[6] De Luca, A., Lanari, L. and Ulivi, G., 1990, "Non-linear Regulation of End-effector Motion for a Flexible Robot Arm," *New Trends in Systems Theory*.

[7] Hirschorn, R. M., 1979, "Invertibility of Multivariable Nonlinear Control Systems," *IEEE Trans. on Automatic Control*, vol.24, no.6, pp.855-865.

[8] Lucibello, P. and Di Benedetto, M. D., 1989, "Exact Tracking with Bounded Elastic Vibration for a Flexible Robot Arm," in *Diagnostics, Vehicle Dynamics and Special Topics ASME Book*, No.H0508E.

[9] Siciliano, B. and Book, W. J., 1988, "A Singular Perturbation Approach to Control Lightweight Flexible Manipulators," *Int. J. Robotics Research*, vol.7, pp.79-90.

[10] Silverman, L. M., 1969, "Inversion of Multivariable Linear Systems," *IEEE Trans. on Automatic Control*, vol.14, no.3, pp.270-276.

[11] Singh, S. N., 1981, "A Modified Algorithm for Invertibility in Nonlinear Systems," *IEEE Transactions on Automatic Control*, vol.AC-26, no.2, pp.595-599.

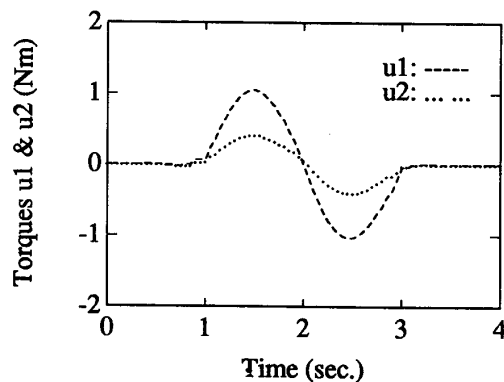


Figure 1: Input Torques

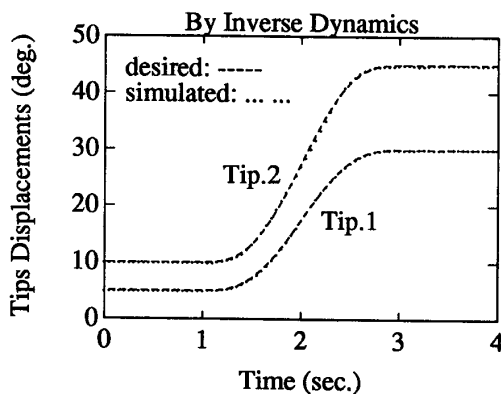


Figure 2: Desired and Simulated Outputs I

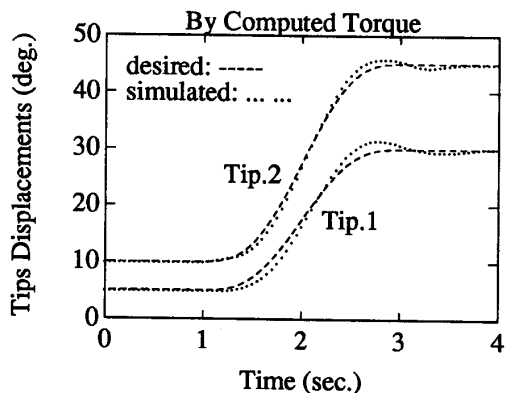


Figure 3: Desired and Simulated Outputs II